Virology 537 (2019) 254–263

Contents lists available at ScienceDirect

Virology

journal homepage: www.elsevier.com/locate/virology

Seneca valley virus activates autophagy through the PERK and ATF6 UPR pathways

Lei Hou[a], Jianguo Dong[b], Shanshan Zhu[a], Feng Yuan[a], Li Wei[a], Jing Wang[a], Rong Quan[a], Jun Chu[a], Dan Wang[a], Haijun Jiang[a], Yanyang Xi[a], Zixuan Li[a], Huiqi Song[a], Yuxin Guo[a], Moran Lv[a], Jue Liu[a,*]

[a] Beijing Key Laboratory for Prevention and Control of Infectious Diseases in Livestock and Poultry, Institute of Animal Husbandry and Veterinary Medicine, Beijing Academy of Agriculture and Forestry Sciences, Beijing, 100097, China
[b] College of Animal Husbandry and Veterinary Medicine, Xinyang Agriculture and Forestry University, Xinyang, 464000, China

ARTICLE INFO

Keywords:
Seneca valley virus
Autophagy
PERK
ATF6
Viral replication

ABSTRACT

Diverse effects on autophagy, a cell degradation pathway, have been associated with the infectious mechanisms of different pathogens. Here, we demonstrated that Seneca valley virus (SVV), an important emerging porcine virus characterized by vesicular lesions and neonatal mortality, can induce autophagy in cultured PK-15 and BHK-21 cells by detecting autophagosome formation, GFP-LC3 puncta and accumulation of LC3-II proteins. Treatment with pharmacological inducers/inhibitors and small interfering RNA sequences targeting genes critical for autophagosome formation affected autophagy induction and viral yields. SVV induced a complete autophagic process to enhance its replication. The PERK and ATF6 pathways, two components of the endoplasmic reticulum (ER)-related unfolded protein response (UPR), were also activated in SVV-infected cells and down-regulation of their expression suppressed SVV-induced autophagy and viral yields. Overall, these results reveal that SVV induces autophagy in cultured cells through the PERK and ATF6 pathways, thereby contributing to understanding of the molecular mechanisms underlying SVV pathogenesis.

1. Introduction

Seneca valley virus (SVV) is a nonenveloped, single-stranded, positive-sense RNA virus within the *Picornaviridae* family (with one species, Senecavirus A) and is most closely related to members of the genus *Cardiovirus* (Hales et al., 2008). SVV infection often results in vesicular lesions on the coronary bands, oral mucosa, snouts, or hooves in pigs, while common clinical signs include lethargy and lameness (Joshi et al., 2016a). Additionally, infection of SVV is clinically manifested by neurological signs, diarrhea and/or sudden death in piglets less than seven days of age (Canning et al., 2016; Joshi et al., 2016b). SVV was originally identified as a contaminant in a cell culture of human fetal retinoblasts in the United States in 2002 and was believed to have been introduced into the cell culture medium via contaminated bovine serum or porcine trypsin (Leme et al., 2017). SVV initially exhibited a putative oncolytic property and was used to treat human cancers (Coffin, 2015). In 2007, SVV infection was detected in pigs with vesicular lesions in Canada (Pasma et al., 2008). To date, a high number of SVV infections, which were determined to be associated with porcine idiopathic vesicular disease, have occurred in pigs in the United States, Brazil and China (Leme et al., 2016; Saeng-Chuto et al., 2018; Sun et al., 2017; Vannucci et al., 2015; Zhao et al., 2017; Zhu et al., 2017). This infection pattern suggests an apparently rapid spread of SVV infection in other countries. In addition, SVV infection of neonatal piglets led often to vesicular lesions and acute death.

Autophagy is an evolutionarily conserved eukaryotic catabolic process that sequesters damaged organelles and long-lived proteins into autophagosomes for lysosomal digestion. The complete autophagic process includes autophagosome formation, autophagosome-lysosome fusion and substrate digestion in lysosomes. During autophagy, microtubule-associated protein 1 light chain 3 (LC3) is converted to lipidated LC3-II, which serves as a marker for autophagy in host cells, by interacting with phosphatidylethanolamine (Kabeya et al., 2000). The multifunctional protein p62, also known as polyubiquitin-binding protein sequestosome 1 (SQSTM1), acts as a substrate for degradation by the autophagy-lysosome pathway, which can be used to assess autophagic flux (Klionsky et al., 2008; Mizushima and Yoshimori, 2007). Autophagy plays a major role not only in cellular homeostasis but also

* Corresponding author.
E-mail address: liujue@263.net (J. Liu).

https://doi.org/10.1016/j.virol.2019.08.029
Received 5 June 2019; Received in revised form 29 August 2019; Accepted 29 August 2019
Available online 30 August 2019

in the response to physiological and pathological factors, such as nutrient starvation and pathogen infection (Klionsky et al., 2008; Tanida, 2011). Recently, many studies have focused on the effect of autophagy on viral replication. Originally, autophagy may provide an antiviral defense strategy against a wide variety of invading viruses (Alexander et al., 2007; García-Valtanen et al., 2014; Yoshimori, 2010). However, some pathogens, such as coxsackievirus, encephalomyocarditis virus (EMCV), Newcastle disease virus (NDV), and avian metapneumovirus (aMPV), have developed various strategies to manipulate autophagy for their own benefit (Hou et al., 2017; Meng et al., 2012; Yoon et al., 2008; Zhang et al., 2011).

The endoplasmic reticulum (ER), which is a multifunctional signaling organelle, controls calcium homeostasis, the folding and oligomerization of newly synthesized proteins and components of redox signaling in eukaryotic cells. However, ER malfunction originates from endogenous imbalances known as ER stress (Kania et al., 2015; Liu et al., 2014). To restore ER homeostasis, activation of the unfolded protein response (UPR) decreases ER loading and enhances folding capacity in cells. Briefly, three UPR pathways, the PKR-like ER protein kinase (PERK) pathway, the activating transcription factor 6 (ATF6) pathway, and the inositol-requiring enzyme 1/X-box binding protein 1 (IRE1/XBP1) pathway, can maintain intracellular homeostasis by dimerization, transfer and autophosphorylation. ER stress and UPR pathways are activated during the viral infection process. Moreover, ER stress can induce autophagy through the activation of the UPR pathways (Yorimitsu et al., 2006). Many viruses in the *Picornaviridae* family have been reported to induce autophagy, which is beneficial for viral replication (Corona Velazquez et al., 2018; Fu et al., 2015; Hou et al., 2014). However, no data showing the involvement of autophagy in SVV infection have yet been reported. Therefore, it is essential that we investigate the relationship and molecular mechanisms connecting SVV infection with the autophagy.

Here, we first demonstrated that a complete autophagic process occurs in SVV-infected host cells and is required for efficient SVV replication. Additionally, we found that the regulation of the PERK and ATF6 UPR pathways plays a major role in the SVV-induced autophagic process and that knockdown of PERK or ATF6 gene expression inhibits SVV replication in cultured host cells.

2. Materials and methods

2.1. Cells cultures and virus

PK-15 cells and BHK-21 cells were originally obtained from the American Type Culture Collection (ATCC CRL-1711 and CRL-1650) and cultured in Dulbecco's modified Eagle's medium (DMEM; Life Technologies, 11995) supplemented with 5–10% fetal bovine serum (FBS, Gibco; Life Technologies, 10099-141).

An SVV strain (CHhb17) maintained in our laboratory was used in this study. Heat-inactivated SVV was kept at 90 °C for 20 min in a water bath, and the infectivity of the inactivated virus was assessed in BHK-21 cells.

2.2. Antibodies and reagents

Rabbit anti-SQSTM1 (P0067), rabbit anti-LC3 (L7543), and mouse anti-β-actin (A5441) primary antibodies, horseradish peroxidase (HRP)-conjugated goat anti-rabbit (A0545) or anti-mouse (A9044) secondary antibodies, tetramethyl rhodamine isothiocyanate (TRITC)-conjugated goat anti-rabbit (T6778) secondary antibody, 3-MA (M9281), Rap (R0395), CQ (C6628) and Tg (T9033) were obtained from Sigma-Aldrich. Mouse anti-GRP78 (3183) and anti-ATG7 (8558) were purchased from Cell Signaling Technology. Rabbit polyclonal antibodies against p-PERK (AP328) were purchased from Beyotime. Antibodies against PERK (sc-377400) and ATF6 precursor (sc-22799) were purchased from Santa Cruz Biotechnology. Rabbit polyclonal antibodies against VP1 were prepared in our laboratory.

2.3. Plasmid construction

The hamster *LC3* gene (RefSeq XM_003495104) was amplified from BHK-21 cells by RT-PCR with gene-specific primers (Table S1) and subcloned into pEGFP-C1 (Clontech, 6084-1) to generate the pEGFP-LC3 expression plasmid. This plasmid was corrected by sequencing.

2.4. Virus infection and titration

PK-15 cells or BHK-21 cells were infected with SVV at a multiplicity of infection (MOI) of 10 or with phosphate-buffered saline (PBS). After 1 h of absorption, the cells were washed two times with PBS and were then incubated at 37 °C for further experiments. BHK-21 cells were pretreated with optimal concentrations of pharmacological compounds for 1 h or 4 h prior to viral infection. SVV-infected BHK-21 cells treated with pharmacological compounds or transfected with siRNA were subjected to two freeze-thaw cycles and were then centrifuged. Viral titers were determined using a plaque assay.

2.5. Silencing LC3, ATG7, PERK and ATF6 gene expression by RNAi

The following siRNAs were designed by GenePharma Company (Suzhou, China): si*LC3* (sense, 5′-GCGUCGCAGCUUCGAATT-3’; antisense, 5′-UUGUUCGAAGCUGCGACGCTT-3′), si*ATG7* (sense, 5′-GCAGUUUGCUCCCUUUAAUTT-3’; antisense, 5′-AUUAAAGGGAGCAAACUGCTT-3′), si*PERK* (sense, 5′-GCACUGGUGGAAGGAAAUATT-3’; antisense, 5′-UAUUUCCUUCCACCAGUGCTT-3′), si*ATF6* (sense, 5′-GCAGCUCCCAAGACUCAAATT-3’; antisense, 5′-UUUGAGUCUUGGGAGCUGCTT-3′) and scrambled siRNA (sense, 5′-UUCUCCGAACGUGUCACGUTT-3’; antisense, 5′-ACGUGACACGUUCGGAGAATT-3′). These siRNAs were transfected with siRNA at a dose of 10–40 pmol using Lipofectamine RNAiMAX (Invitrogen, 13778) according to the manufacturer's protocol. The silencing efficiency of *ATG7*, *LC3*, *PERK* or *ATF6* siRNA in BHK-21 cells was further assessed after 48 h.

2.6. RNA preparation and RT-PCR analysis

Total RNA was prepared from BHK-21 cells with a RNeasy Mini Kit (Qiagen, 74104) according to the manufacturer's protocol. Two micrograms of RNA were reverse transcribed into cDNA for further experiments.

The *XBP1* gene (Ref Seq NM_001244049) and glyceraldehyde-3-phosphate dehydrogenase (*GAPDH*) gene (Ref Seq NM_001244854) were amplified from BHK-21 cells with specific primers (Table 1).

2.7. Sodium dodecyl sulfate-polyacrylamide gel electrophoresis (SDS-PAGE) and Western blot assay

After infection or transfection, BHK-21 cells were lysed with RIPA lysis buffer (Beyotime, P0013B) containing 1 mM

Table 1
Primers used for amplifying the *LC3*, *XBP1* and *GAPDH* genes.

Primer[a]	Sequence (5′–3′)[b]	Size (bp)
*LC3*F	CTGAATTCTATGCCGTCCGAGAAGACCT (*Eco*R I)	378
*LC3*R	ATGTCGACTTACACAGCCATTGCTGTC (*Sal* I)	
*XBP1*F	AAACAGAGTAGCAGCGCAGACTGC	598
*XBP1*R	GGATCTCTAAGACTAGAGGCTTGGTG	
*GAPDH*F	GTGGAAGTTGTTGCCATCAATGA	136
*GAPDH*R	CTCCTGGAAGATGGTGATGGC	

[a] F denotes a forward PCR primer; R denotes a reverse PCR primer.
[b] The restriction sites are underlined and specified in parentheses at the end of the sequence.

phenylmethanesulfonyl fluoride (PMSF) (Beyotime, ST506-2) and centrifuged. The protein concentration in the supernatant was determined using a bicinchoninic acid (BCA) protein assay kit (Thermo Scientific, 23225). Twenty micrograms of protein were separated using SDS-PAGE and transferred to nitrocellulose membranes (Pall, 66485). After blocking with 5% non-fat milk for 2 h at room temperature (RT), the membranes were subsequently reacted with primary antibodies at RT for 2 h, followed by HRP-conjugated secondary antibodies at RT for 2 h. Proteins on the membranes were detected using a SuperSignal West Pico PLUS Chemiluminescent Substrate Kit (Thermo Scientific, 34580) and visualized via a chemiluminescence apparatus (ProteinSimple, Santa Clara, CA, USA).

2.8. Confocal microscopy

BHK-21 cells cultured to a confluence of approximately 70–80% were transfected with pEGFP-LC3 plasmids for 12 h in 24-well culture plates and were then infected with SVV. The cells were fixed with 4% paraformaldehyde (Sigma-Aldrich, 16005) for 15 min and then permeabilized with 0.1% Triton X-100 (Sigma-Aldrich, T8787) for 15 min. A rabbit anti-VP1 polyclonal antibody and secondary TRITC-conjugated anti-rabbit antibodies were sequentially incubated at 37 °C for 2 h each. Following washing with PBS, fluorescent images were obtained using a Nikon AIR confocal immunofluorescence microscope (Nikon Instruments, Inc., Melville, NY, USA).

2.9. TEM

For TEM, BHK-21 cells were infected with SVV for 24 h and processed as previously described [18]. The localization of SVV proteins or particles in virus-infected BHK-21 cells was detected via immunoelectron microscopy (IEM) with the preembedding silver enhancement immunogold method (Mizushima et al., 2001). Frozen ultrathin sections were processed and subsequently incubated with an anti-VP1 antibody (1000 ×) followed by goat anti-rabbit IgG (100 ×) conjugated to colloidal gold particles (Sigma, G7402). Finally, the ultrathin sections were incubated with a silver enhancement kit (Sigma, SE100) and then images were obtained using a Hitachi H-7500 transmission electron microscope (Hitachi Ltd, Japan).

2.10. Statistical analysis

Data are expressed as the means ± standard deviations (SDs) and were compared by one-way analysis of variance (ANOVA), Dunnett's and Tukey's post hoc tests and two-way ANOVA. P values of < 0.05 were considered statistically significant.

3. Results

3.1. SVV infection induces autophagy in host cells

Transmission electron microscopy (TEM), a standard method, can be used to monitor the morphology of autophagic compartments and observe the formation of autophagic vacuoles (Klionsky et al., 2016; Tanida, 2011). Thus, to investigate whether SVV infection triggers ultrastructural changes, an ultrastructural analysis was performed in SVV-infected BHK-21 cells. SVV-infected cells had noticeably more single- or double-membraned vesicles in the cytoplasm than uninfected (mock-infected) cells at 24 h post infection (hpi). Moreover, most of the autophagic SVV-infected cell vacuoles with typical morphologically characteristics contained recognizable degraded organelles or cytoplasmic contents, whereas uninfected cells showed normal organelles or dense cytoplasmic contents (Fig. 1A, panels a and b). We further confirmed the sites of SVV replication in the vesicles. The signal from anti-VP1 protein immunogold labels incubated with anti-VP1 antibodies, which likely represented viral proteins or virions, was mainly localized on vesicular membranes (Fig. 1A, arrowheads in panel c). In contrast, in mock-infected BHK-21 cells, rabbit immunoglobulin G was gold-labeled with anti-VP1 antibody incubation but no positive signals were observed (data not shown). In addition, no signal from immunogold labels was seen in negative control cells incubated without primary antibody (data not shown). Overall, these results strongly suggest that the number of autophagosome-like vesicles was significantly increased in SVV-infected BHK-21 cells and that the site of SVV replication mainly appeared on the vesicle membranes.

To further verify that the formation of autophagosome-like vesicles is related to autophagy in SVV-infected cells, we examined the accumulation of the LC3-II protein, a marker protein of autophagy, using Western blot analysis (Klionsky et al., 2016; Mizushima and Yoshimori, 2007). The accumulation of LC3-II gradually increased from 0 to 48 h after SVV infection, whereas mock-infected BHK-21 cells did not exhibit significant conversion of LC3 (Fig. 1B, upper panel). In addition, VP1 protein expression represented the progression of SVV infection (Fig. 1B, upper panel). Similarly, LC3-II accumulation was also observed in PK-15 cells during the 0–48 hpi period (Fig. 1B, lower panel). As shown in Fig. 1B, beginning at 12 hpi, the densitometric ratio of the β-actin and LC3-II bands, an accurate indicator of autophagic activity, was much higher in SVV-infected BHK-21 and PK-15 cells than in the corresponding mock-infected BHK-21 cells, indicating that SVV infection promotes a gradual increase in the formation of autophagosome-like vesicles ($P < 0.01$). More importantly, accompanied by the accumulation of LC3-II, the VP1 protein expression increased in SVV-infected host cells (Fig. 1B). These results confirm that SVV infection clearly induces autophagy in PK-15 and BHK-21 cells.

The accumulation of LC3 protein puncta, another marker of autophagosome-like vesicle formation, indicates the recruitment of LC3-II to autophagic vacuoles (Klionsky et al., 2016). BHK-21 cells were transfected with green fluorescent protein (GFP) fused to LC3 (GFP-LC3), which facilitated the observation of autophagosome-like vesicles by confocal immunofluorescence microscopy. The green fluorescence displayed a punctate pattern after SVV infection, as evidenced by the positive red VP1 protein staining. In contrast, the GFP-LC3 signal was diffuse and the puncta were rarely observed in mock-infected cells (Fig. 1C, $P < 0.01$). These results demonstrate that SVV infection induces the formation of autophagosomes.

Heat-inactivated viruses are considered to lose replication activity (Hu et al., 2015). Thus, to analyze whether SVV replication is indispensable for autophagy, we evaluated the conversion of LC3 in heat-inactivated virus-infected BHK-21 cells. The loss of viral infectivity by heat treatment was detected by indirect immunofluorescence assay (data not shown). LC3-II expression in heat-inactivated SVV-infected cells at 24 hpi was similar to that in mock-infected cells, in which LC3-II expression decreased to marginal levels (Fig. 1D). Moreover, no VP1 protein was observed in the heat-inactivated SVV-infected cells, indicating that the replication of SVV is required for the activation of autophagy.

3.2. Autophagy influenced by Rap or 3-MA regulates SVV replication

To confirm the relationship between autophagy and SVV replication, SVV-infected cells were treated with autophagy regulators, 3-methyladenine (3-MA) or rapamycin (Rap) (Noda and Ohsumi, 1998), to evaluate virus production. As shown in Fig. 2, compared to untreated cells, Rap-treated cells exhibited noticeable increases in the LC3-II protein accumulation ($P < 0.001$), VP1 protein expression ($P < 0.001$) and viral yields ($P < 0.05$) at 24 hpi (Fig. 2A–B). In contrast, the intensity of the LC3-II bands and the expression of the VP1 protein were significantly decreased upon 3-MA treatment compared with those levels in the SVV-infected cells without 3-MA treatment (Fig. 2C, $P < 0.001$), and 3-MA-treated cells exhibited an appreciable decline at 24 hpi (Fig. 2D, $P < 0.05$). Moreover, the viability of pharmacologically treated cells and untreated cells was not clearly

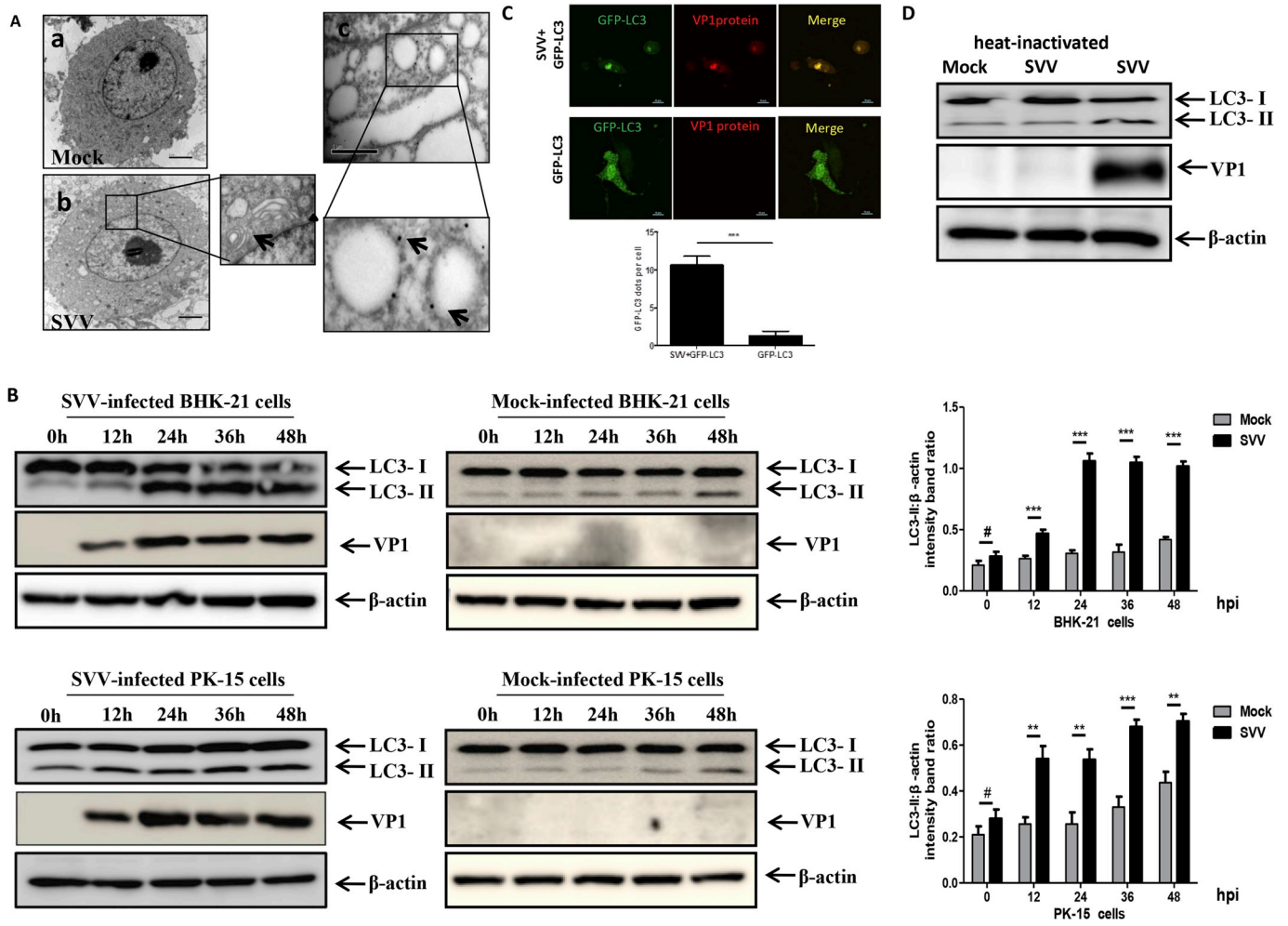

Fig. 1. SVV infection triggers autophagy in PK-15 and BHK-21 cells. (A) Autophagic vacuoles in SVV-infected or mock-infected BHK-21 cells were observed with TEM at 24 hpi (panels a and b). The frozen ultrathin sections were incubated with an anti-VP1 antibody and a secondary antibody conjugated to colloidal gold particles for TEM observation (panel c). The autophagosome-like vesicles and colloidal gold particles are indicated by black arrowheads. Scale bars, 1–2 μm. (B) SVV-infected or mock-infected BHK-21 or PK-15 cells were processed at 0, 12, 24, 36 and 48 hpi, and extracted proteins were subjected to Western blotting with anti-VP1 and anti-LC3 antibodies. β-actin was used for a protein loading control. Quantification displayed with graphs representing the LC3-II/β-actin band ratios normalized to the control condition. (C) BHK-21 cells were transfected with pGFP-LC3 plasmids. After 12 h, cells were infected with SVV and observed with GFP-LC3 puncta (green) and viral VP1 protein staining (red) by confocal immunofluorescence at 24 hpi. Scale bars, 10 μm. GFP-LC3 expression signal was counted in the cells. (D) Replication-competent SVV- or heat-inactivated SVV-infected BHK-21 cells were harvested, processed and analyzed at 24 hpi as described in (B). Error bars: means ± SDs of three independent tests. Two-way ANOVA; $^{\#}P > 0.05$, $^{**}P < 0.01$, $^{***}P < 0.001$ compared to the control group. (For interpretation of the references to colour in this figure legend, the reader is referred to the Web version of this article.)

different according to the MTT assay results (data not shown). These results finally demonstrate that autophagy has a crucial effect on SVV replication.

3.3. Knockdown of endogenous ATG7 or LC3 gene expression inhibits SVV replication

To extend the effects of autophagy on viral replication, we conducted experiments to further analyze the effect of knocking down the expression of the autophagy-related proteins autophagy-related 7 (ATG7) and LC3 via target-specific RNA interference (RNAi) on SVV replication in cells. The autophagy proteins ATG7 and LC3 are required for autophagosome formation (Komatsu et al., 2005; Hou et al., 2017). BHK-21 cells transfected with small interfering RNA (siRNA) targeting *ATG7* or *LC3* exhibited a dose-dependent reduction in protein expression (Fig. 3A). Ultimately, 30 pmol of transfected siRNA was used for subsequent experiments. Further experiments showed that cells with knockdown of endogenous *ATG7* or *LC3* gene expression exhibited significant decreases in VP1 protein expression (Fig. 3B–C, $P < 0.001$) and viral titers at 24 hpi (Fig. 3D–E, $P < 0.05$). Taken together, these results further confirm that autophagy is indispensable for the active SVV replication.

3.4. Complete autophagy induced by SVV is beneficial for viral replication

The p62 (SQSTM1) protein is degraded by lysosomal hydrolases during autophagosome maturation (Klionsky et al., 2016; Mizushima et al., 2010), which is defined as a complete autophagic process that triggers autophagic flux. To evaluate whether a complete autophagic process is induced in SVV-infected cells, we assessed SQSTM1 expression in cultured cells by Western blot analysis (Fig. 4A). SVV infection resulted in a gradual decrease in SQSTM1 expression from 0 to 48 hpi, whereas SQSTM1 expression did not noticeably change in mock-infected cells, suggesting that SVV infection induced autophagic flux in cultured cells.

To further confirm whether SVV infection induced a complete autophagic process, we added chloroquine (CQ), a specific inhibitor of autophagosome-lysosome fusion (Boya et al., 2005; Klionsky et al.,

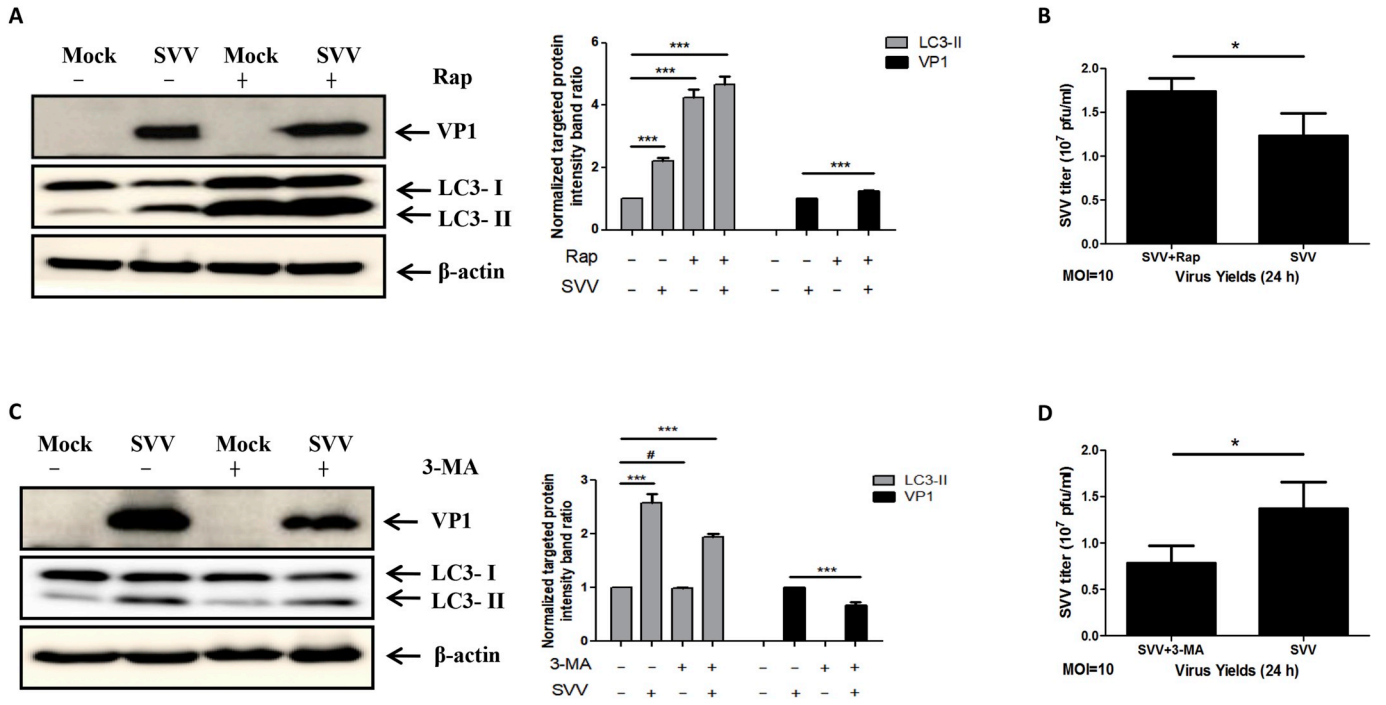

Fig. 2. The effect of pharmacological compounds on SVV replication via autophagy. (A) BHK-21 cells were treated or mock treated with 100 nM Rap. After 4 h, cells were infected with SVV and further cultured for 24 h with or without Rap. The extracted proteins were analyzed by Western blotting when reacted with anti-VP1 and anti-LC3 antibodies. The Rap treatment is denoted by a "+". Quantification displayed with graphs representing the LC3-II/β-actin or VP1/β-actin ratios normalized to the control condition. (B) BHK-21 cells were treated as described in (A). Virus titers were determined by a plaque assay at 24 hpi. (C) BHK-21 cells were treated or mock treated with 2.5 mM 3-MA. After 4 h, cells were infected with SVV and further cultured for 24 h with or without 3-MA. The extracted proteins were analyzed as described in the legend of Fig. 2A. The treatment of 3-MA is denoted by a "+". Quantification shown with graphs representing the LC3-II/β-actin or VP1/β-actin ratios normalized to the control conditions. (D) Virus productions were detected as described in (B). Error bars: means ± SDs of three independent experiments. Two-way ANOVA; $^{\#}P > 0.05$, $^{*}P < 0.05$, $^{***}P < 0.001$ compared to the control group.

2016), to SVV-infected and mock-infected cells to investigate LC3 protein conversion and autophagic flux. As shown in Fig. 4B, SVV-infected BHK-21 cells treated with CQ exhibited a significant increase in an accumulation of LC3-II and a reversal of SQSTM1 downregulation compared to mock-infected cells ($P < 0.05$). As expected, the viral VP1 protein expression and viral yields in CQ-treated cells were appreciably reduced compared to those in SVV-infected cells at 24 hpi (Fig. 4B–C, $P < 0.001$). Additionally, the viability of BHK-21 cells treated with CQ was not clearly affected using the MTT assay (data not shown). Overall, these results indicate that the complete autophagic process induced by SVV is beneficial for viral production.

3.5. SVV infection induces the PERK and ATF6 UPR signals in response to ER stress

To elucidate the mechanism of SVV-induced autophagy, we investigated whether SVV infection induces ER stress and UPR pathways in BHK-21 cells, as the abovementioned factors have been reported to induce autophagy (Hou et al., 2014; Wang et al., 2014; Yamamoto et al., 1998). The 78 kDa glucose-regulated protein (GRP78), which is an ER stress marker protein, mainly reflects the degree of ER stress. As expected, both thapsigargin (Tg) treatment and SVV infection increased the expression of GRP78 compared with that in control BHK-21 cells (Fig. 5A). Moreover, compared to mock-infected cells, the Tg-treated or SVV-infected cells showed a noticeable increase in the conversion of LC3, suggesting that ER stress can trigger autophagy in SVV-infected BHK-21 cells.

To alleviate ER stress, we investigate the UPR pathway by which SVV infection induces autophagy. We first analyzed the phosphorylation of PERK to examine whether the PERK pathway was activated in SVV-infected BHK-21 cells. As shown in Fig. 5A, cells treated with Tg and infected with SVV exhibited much higher expression levels of phosphorylated (p)-PERK than control cells. Second, under stress conditions, ATF6 is cleaved and transferred to the nucleus, where it finally induces the expression of many genes to alleviate the ER stress response (Haze et al., 1999; Shen et al., 2002). Thus, ATF6 cleavage was examined to assess whether SVV infection activates the ATF6 pathway. As shown in Fig. 5A–B, both Tg treatment and SVV infection appreciably increased ATF6 degradation, and SVV infection resulted in a gradual increase in cleaved ATF6 (50 kDa) expression from 0 to 48 hpi. These results demonstrate that SVV infection can activate the PERK and ATF6 pathways in BHK-21 cells.

Activation of the IRE1-XBP1 pathway could cause *XBP1* mRNA splicing. Digestion occurred at the unique *Pst* I restriction of *XBP1* cDNA, indicating activation of the IRE1-XBP1 signal, as previously described (Fig. 5C) (Yu et al., 2006; Zhang et al., 2010). To verify whether SVV infection induced autophagy via the IRE1-XBP1 pathway in BHK-21 cells, amplified *XBP1* cDNA by RT-PCR was digested with *Pst* I. Tg was used as the positive control for inducing *XBP1* splicing (*XBP1s*). As shown in Fig. 5D, the intensity of the *XBP1s* bands in the Tg-treated cells was much stronger than those in the mock-infected cells and SVV-infected cells, as shown by the inhibition of *XBP1* cDNA splicing to *Pst* I digestion. However, the levels of *XBP1* in SVV-infected cells and mock-infected cells did not appreciably differ. To further confirm this result, we assessed the intensity of the *XBP1s* bands at different time points (0–48 h) after SVV infection by RT-PCR and digestion with *Pst* I (Fig. 5E). No obvious differences were observed in the levels of *XBP1* after SVV infection. These results indicate that the IRE1-XBP1 signal was not activated via *XBP1* splicing in SVV-infected cells.

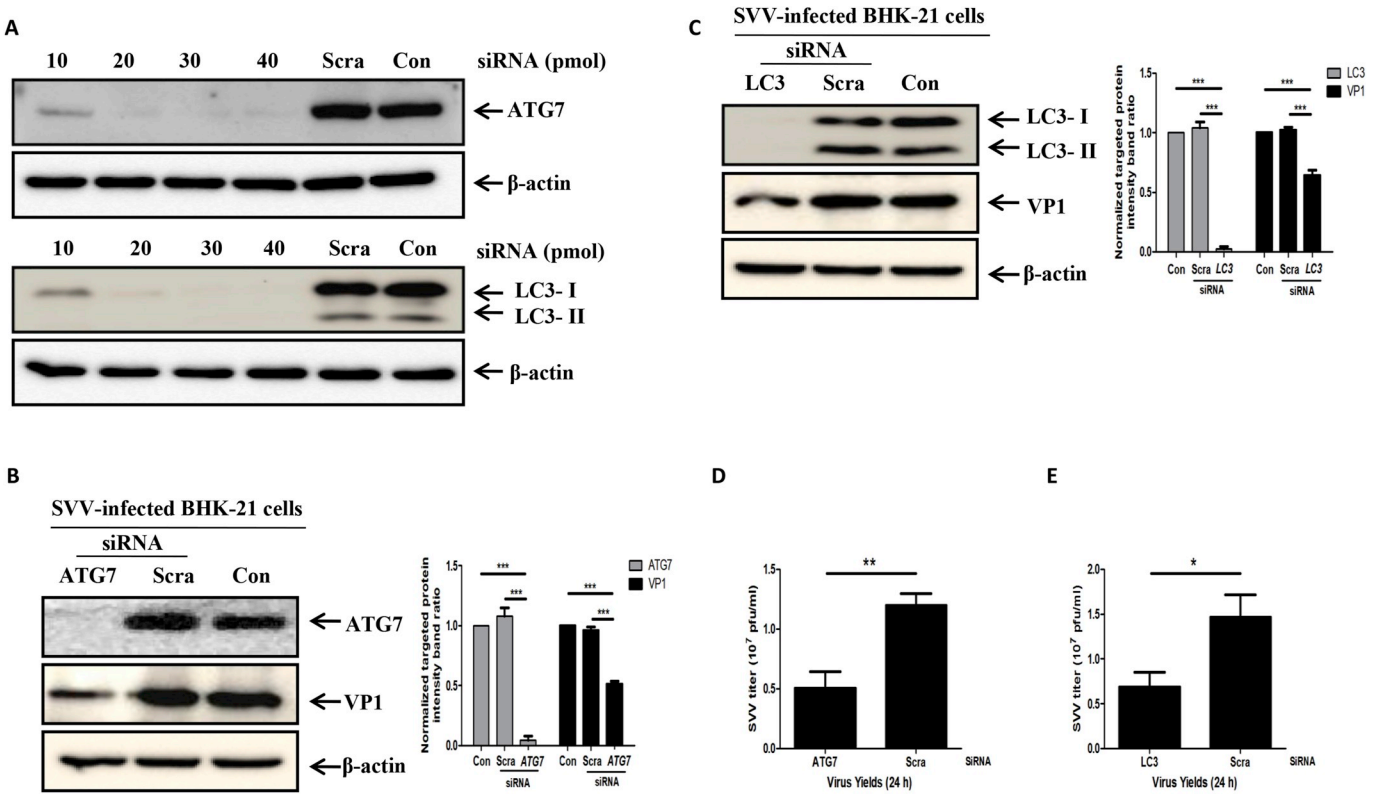

Fig. 3. Silencing *ATG7* or *LC3* gene expression inhibits SVV replication. (A) BHK-21 cells were mock transfected (Con) or transfected with 10, 20, 30 or 40 pmol of *ATG7*-siRNA or *LC3*-siRNA or with 40 pmol scramble-siRNA (Scra) for 48 h. ATG7 and LC3 protein expression was assessed by Western blotting. (B) BHK-21 cells were transfected with siRNA targeting *ATG7* or Scra. After 48 h, cells were infected with SVV and were further subjected to Western blotting to analyze the ATG7, VP1 and β-actin expression levels at 24 hpi. Quantification shown with graphs representing the ATG7/β-actin or VP1/β-actin ratios normalized to the control conditions. (C) BHK-21 cells were transfected with siRNA targeting *LC3* or Scra. Cells were processed as described in (B) and analyzed with anti-LC3, anti-VP1 and anti-β-actin antibodies at 24 hpi. Quantification shown with graphs representing the LC3-II/β-actin or VP1/β-actin ratios normalized to the control condition. (D) BHK-21 cells were treated as described in (B). Virus titers were detected by a plaque assay at 24 hpi in BHK-21 cells. (E) BHK-21 cells were treated as described in (C). Virus titers were detected by a plaque assay at 24 hpi in BHK-21 cells. Error bars: means ± SDs of three independent experiments. Two-way ANOVA; $^*P < 0.05$, $^{**}P < 0.01$, $^{***}P < 0.001$ compared to the control group.

3.6. Knockdown of endogenous PERK or ATF6 gene expression inhibits viral replication

To confirm whether autophagy was induced through the PERK and ATF6 UPR pathways in SVV-infected BHK-21 cells, we examined the effect of silencing endogenous *PERK* or *ATF6* gene expression on SVV-induced autophagy and viral yields. First, BHK-21 cells transfected with *PERK* or *ATF6* siRNA exhibited a dose-dependent reduction in protein expression (Fig. 6A); a 40 pmol dose of siRNA was ultimately used for further study. Next, compared to scrambled siRNA-transfected cells and control cells, cells with knockdown of the *PERK* or *ATF6* gene exhibited decreased SVV-induced LC3 conversion and viral VP1 protein expression (Fig. 6B–C). Similarly, viral yields were noticeably decreased at 24 hpi in BHK-21 cells with knockdown of PERK or ATF6 (Fig. 6D–E, $P < 0.05$). These results indicate that silencing the *PERK* or *ATF6* genes by siRNA can inhibit induction of autophagy and viral replication in SVV-infected BHK-21 cells.

4. Discussion

Autophagy is a cellular physiological process that plays a crucial role in maintaining cellular homeostasis and coordinating the cellular response to pathogen infection. Many reports have focused on the effect of autophagic induction on the replication of *Picornaviridae* family members and the underlying induction mechanisms (Alirezaei et al., 2015; Fan et al., 2017; Hou et al., 2014). However, to date, little is known regarding the mechanism of autophagy in SVV-infected cells. In this study, we demonstrated that SVV infection successfully triggered autophagy and that autophagy promotes viral replication through the PERK and ATF6 UPR pathways in these cells.

First, our electron microscopy analysis demonstrated that a large number of membrane vesicles induced by SVV infection appeared in BHK-21 cells (Fig. 1A). Moreover, a few immunogold labels were observed around the edges of the single- or double-membrane vesicles, confirming that autophagic vesicles are formed in SVV-infected BHK-21 cells (Fig. 1A). Furthermore, two hallmarks of autophagy, GFP-LC3 puncta formation and LC3 conversion, were further evaluated to assess autophagy induction. The formation of GFP-LC3 protein puncta was observed in SVV-infected cells, and these puncta were colocalized with viral VP1 proteins indicating SVV virions (Fig. 1B). However, GFP-LC3 puncta do not completely imply autophagosome formation (Klionsky et al., 2016). Therefore, to further investigate this possibility, we also assessed the conversion of LC3 via Western blot analysis. The accumulation of LC3-II indicated a significant increase in the autophagy level (Fig. 1B–C). Importantly, beginning at 24 hpi, clear conversion of LC3-II was observed; therefore, we primarily chose this time point for further analysis of SVV-induced autophagic mechanisms. The results of additional experiments in heat-inactivated SVV-infected BHK-21 cells suggested that SVV replication is indispensable for autophagy induction (Fig. 1D).

To understand the relationship between SVV replication and autophagy, we analyzed viral replication through treatment with autophagy regulators or silencing crucial genes in autophagy pathways. First, the induction or inhibition of autophagy with Rap or 3-MA is beneficial

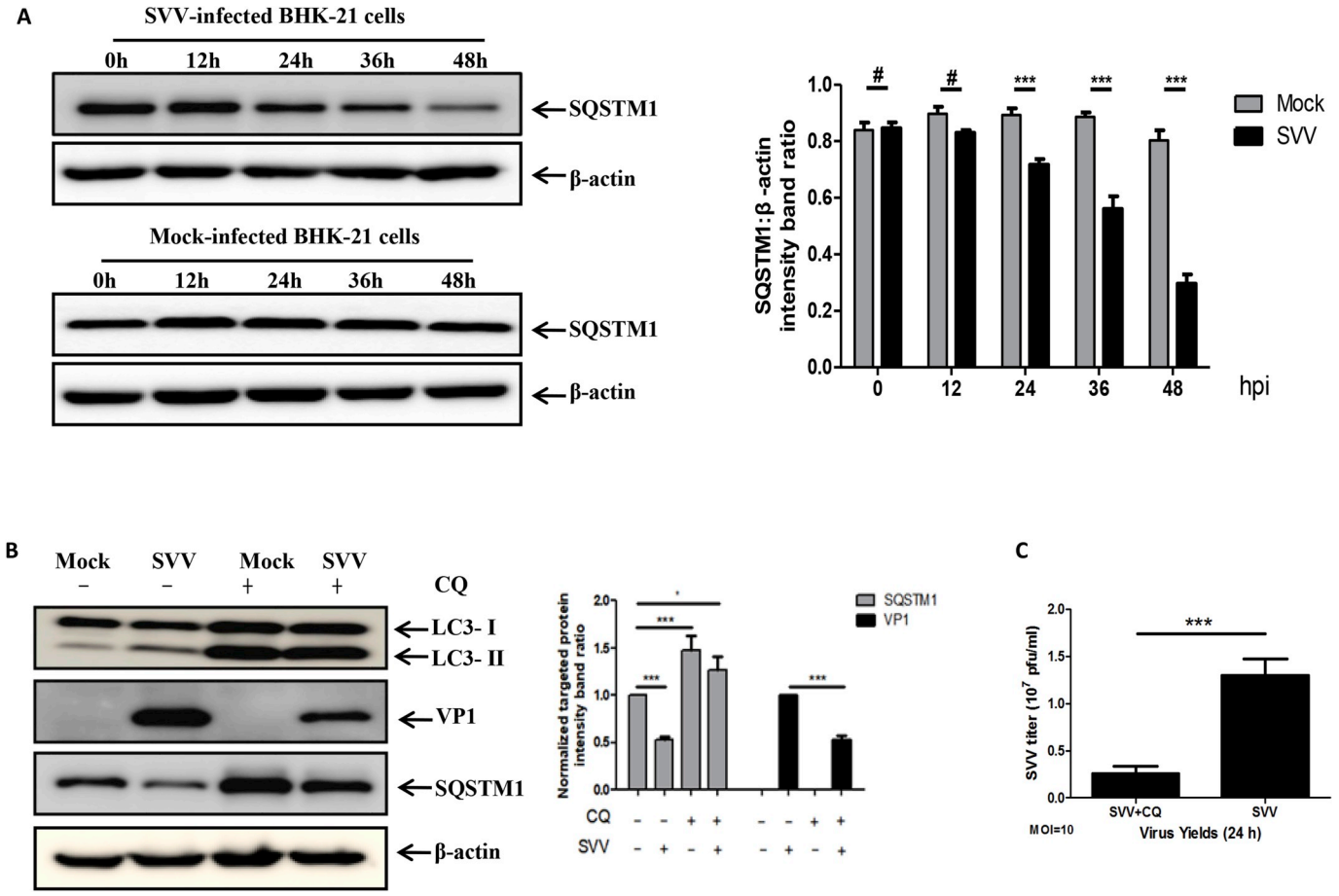

Fig. 4. SVV-triggered complete autophagy facilitates viral replication. (A) SVV-infected or mock-infected BHK-21 cells were processed at 0, 12, 24, 36 or 48 h. SQSTM1 and β-actin protein expression was analyzed by Western blotting. The SQSTM1/β-actin ratio was normalized to the control condition. (B) BHK-21 cells were treated or mock treated with 40 μM CQ. After 1 h, cells were infected with SVV and further cultured for 24 h with or without CQ. The extracted proteins were subjected to Western blotting with anti-VP1 and anti-LC3 antibodies. The CQ treatment is denoted by a "+". Quantification shown with graphs representing the LC3-II/β-actin or VP1/β-actin ratios normalized to the control condition. BHK-21 cells were treated as described in (B). Virus titers were detected by a plaque assay at 24 hpi. Error bars: means ± SDs of three independent experiments. Two-way ANOVA; $^{\#}P > 0.05$, $^{*}P < 0.05$, $^{***}P < 0.001$ compared to the control group.

or detrimental, respectively, to SVV replication and viral yields in BHK-21 cells (Fig. 2). The data are consistent with those of previous studies of autophagy in cells infected with other viruses, such as EMCV (Zhang et al., 2011), NDV (Meng et al., 2012), and aMPV (Hou et al., 2017). Additionally, further analysis showed that the inhibition of autophagosome formation through the knockdown of *ATG7* or *LC3* gene expression decreased SVV replication and viral yields (Fig. 3). Taken together, our results show that autophagy plays an important role in SVV replication and enhances viral yields and viral protein synthesis.

In fact, as a lysosome-dependent complete autophagic process, enhanced autophagy has as one of its important outcomes and hallmarks an increase in autophagic cargo degradation (Liu et al., 2014). For example, hepatitis C virus (HCV) and aMPV have been reported to induce complete autophagy and increase autophagic flux (Hou et al., 2017; Wang et al., 2014). However, previous studies failed to detect this effect in some virus-infected cells (Liu et al., 2014; Sir et al., 2010). As a lysosome-dependent signal, the degradation of SQSTM1 proteins is a crucial decision factor in complete autophagy. Here, we demonstrated that SVV infection triggers a complete autophagic process (Fig. 4). SQSTM1 proteins were degraded in SVV-infected cells (Fig. 4A). To verify whether cleaved SQSTM1 products appeared in the SVV-infected cells, we detected cleaved SQSTM1 products (approximate 31 kDa) using Western blotting. The results showed that no cleaved products were observed in SVV-infected cells (data not shown). This result is different from some other picornaviruses (coxsackievirus B3, Poliovirus and Enteroviruses D68)-mediated cleavage of SQSTM1 (Corona et al., 2018; Corona Velazquez et al., 2018; Mohamud et al., 2019), which may be attributed to characteristics of protease 2A among various picornaviruses. Interestingly, SVV 2A protein only contains nine amino acids, which may lose some function of the protease compared with other picornaviruses 2A proteins. Moreover, SQSTM1 protein degradation was decreased in CQ-treated SVV-infected BHK-21 cells, and these cells exhibited inhibited viral protein synthesis and reduced viral yields. Taken together, these data indicate that SVV infection induces autophagosomal maturation via the enhancement of autophagic flux.

The ER is the major eukaryotic organelle involved in protein folding and maturation. However, dysfunction of the ER, known as ER stress, originates from endogenous imbalances, especially during the viral infection process. The GRP78 protein is a molecular marker of ER stress (Benali-Furet et al., 2005). In the current study, GRP78 protein expression was clearly enhanced in SVV-infected BHK-21 cells (Fig. 5A), indicating that SVV infection triggers ER stress. In the adverse effects of ER stress, the UPR pathways were activated to minimize ER dysfunction. Here, we found that the PERK and ATF6 pathways but not the IRE1/XBP1 pathway were activated (Fig. 5) in SVV-infected BHK-21 cells; this effect also occurred in HCV- or EMCV-infected cells (Hou et al., 2014; Wang et al., 2014), indicating that the PERK and ATF6 pathways play a major role in the infection process of multiple viruses. Our subsequent results confirmed that silencing *PERK* or *ATF6* gene expression inhibits LC3 conversion and SVV replication (Fig. 6). In fact,

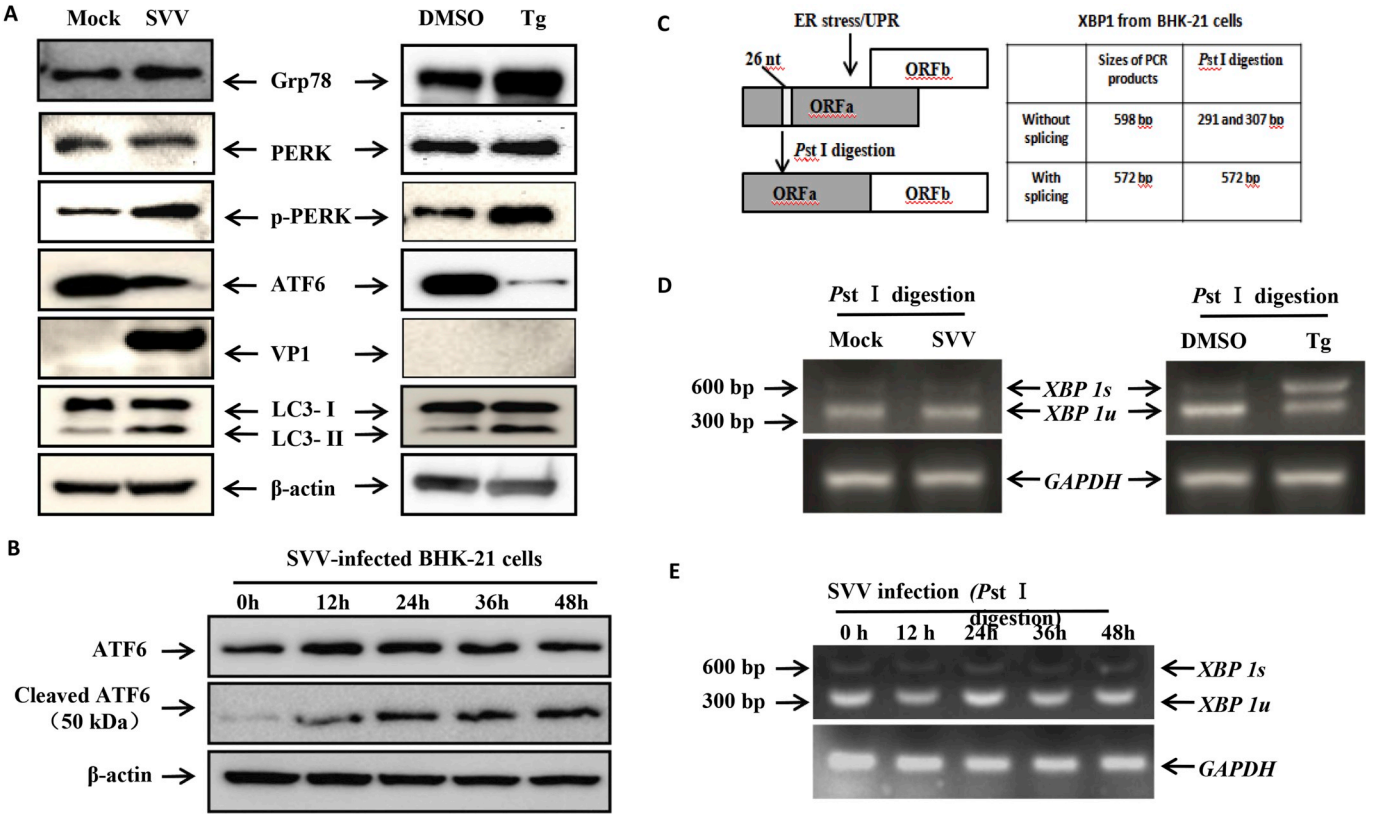

Fig. 5. SVV infection activates the PERK and ATF6 UPR pathways. (A) BHK-21 cells were infected with SVV for 24 h and treated with Tg (500 nM) for 12 h as the positive control. GRP78, PERK, p-PERK, ATF6, LC3, VP1 and β-actin protein expression was analyzed by Western blotting. (B) SVV-infected BHK-21 cells at 0, 12, 24, 36, or 48 hpi were processed for detection of ATF6, cleaved ATF6 (50 kDa), and β-actin protein expression by Western blotting. (C) Schematic illustration of *XBP1* mRNA splicing. The label area indicates the 26-nt intron sequence, the two open reading frames (ORFs) and the *Pst* I restriction site. The sizes of the RT-PCT amplified fragments from the unspliced *XBP1* (*XBP1u*) mRNA and spliced *XBP1* (*XBP1s*) mRNA with or without *Pst* I cleavage are also indicated. (D) BHK-21 cells were treated as described in (A). Electrophoretic analysis showed that the amplified fragments digested with *Pst* I contain *XBP1u* (291/307 bp) and *XBP1s* (572 bp) bands. (E) SVV-infected BHK-21 cells at 0, 12, 24, 36, or 48 hpi were treated as described in (A). Electrophoretic analysis showed that the amplified fragments digested with *Pst* I contain *XBP1u* (291/307 bp) and *XBP1s* (572 bp) bands.

the ER stress and UPR pathway-induced autophagy is characterized by the formation of autophagosomes at different stages, such as induction, vesicle nucleation and vesicle elongation (Song et al., 2018). Therefore, which stages of the PERK and ATF6 pathways involved in autophagic vesicle formation need further determination. Taken together, the results of our studies demonstrate that SVV infection induces autophagy through ER stress-associated PERK and ATF6 UPR signaling and that these two pathways are beneficial for SVV replication.

In addition, importantly, although many *Picornaviridae* family members have a similar genome organization and a similar genomic RNA replication strategy (Hales et al., 2008), not all exhibit shared features in the viral infection process, suggesting that there are many mechanistic differences between SVV and other picornaviruses. First, regarding the autophagosome-lysosome fusion pattern, cells treated with bafilomycin A1, an inhibitor of autophagosome-lysosome fusion (Liang et al., 2008), did not affect foot-and-mouth disease virus (FMDV) replication, indicating that autophagosome-lysosome fusion is dispensable for FMDV replication; such an autophagic process is termed an incomplete process (Gladue et al., 2012). However, for SVV replication, a complete autophagic process including fusion of autophagosomes with lysosomes enhanced viral yields and viral protein synthesis. Second, regarding ER stress-associated UPR pathways, coxsackievirus A16 (CA16) infection activated all three UPR pathways to alleviate ER stress (Zhu et al., 2013), but SVV induced autophagy only through the PERK and ATF6 pathways, which benefited its replication. Considering the uniqueness of the viruses in the *Picornaviridae* family, further studies are needed to investigate and ultimately unveil the mechanistic differences between SVV and other picornaviruses in the autophagosome-lysosome fusion patterns and ER stress-associated UPR pathways.

In conclusion, our results demonstrated for the first time that infection with SVV induced a complete autophagic process, which was regulated by ER stress in BHK-21 cells to some extent. Our results further demonstrated that the PERK and ATF6 UPR pathways are involved in autophagic induction and that reducing PERK or ATF6 expression inhibits SVV replication. These results provide new insight into SVV-induced autophagy in PK-15 and BHK-21 cells and offer additional experimental evidence to advance the understanding of the molecular mechanisms underlying SVV pathogenesis.

Conflicts of interest

The authors declare no potential conflicts of interest.

Acknowledgements

The authors wish to thank Miss Ying Wang of Institute of Food Science and Technology Chinese Academy of Agricultural Sciences Electronic Microscopy facility for technical support in TEM imaging. This study was supported by funds from the National Key Research and Development Program of China (2017YFD0500103) and Key and Cultivation Discipline of Xinyang Agriculture and Forestry University (ZDXK201702).

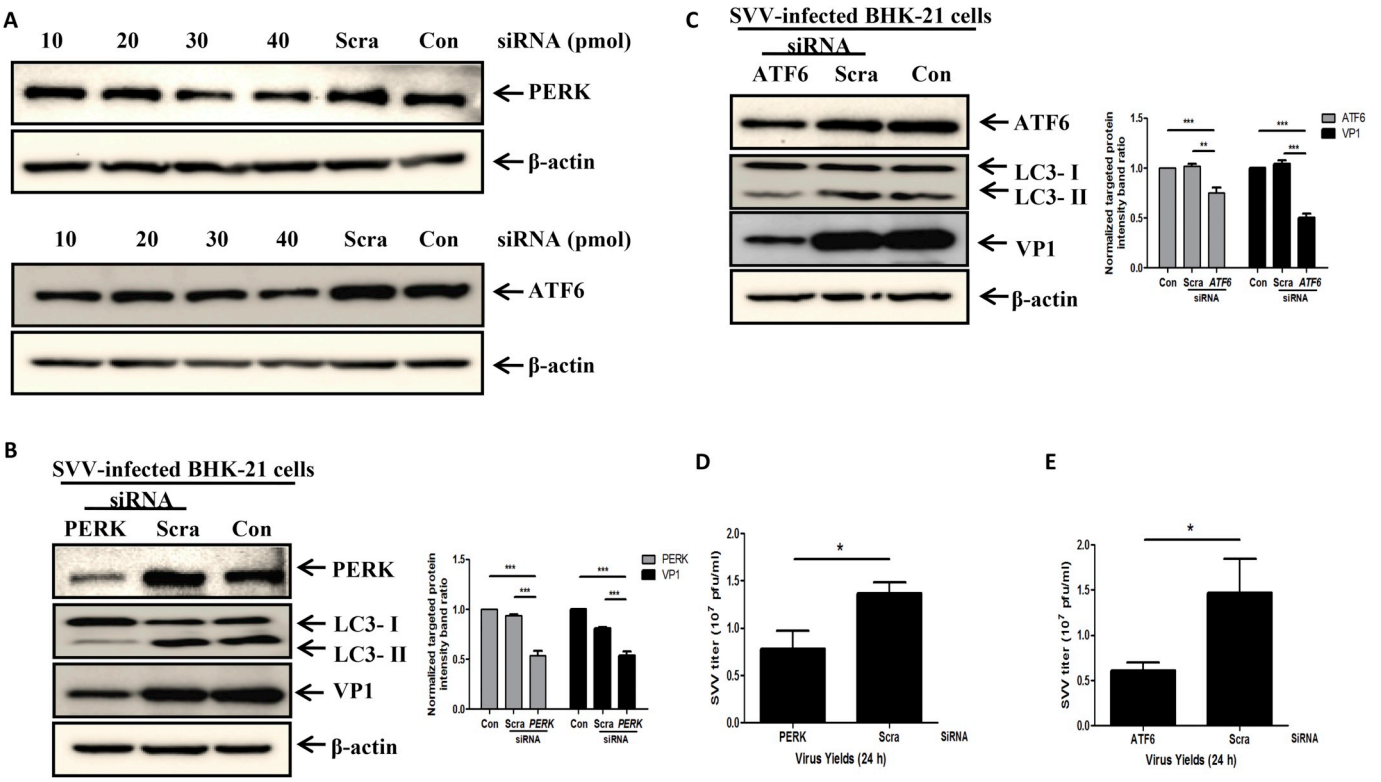

Fig. 6. Silencing *PERK* or *ATF6* gene expression inhibits SVV-induced autophagy and virus production. (A) BHK-21 cells were mock transfected (Con) or transfected with 10, 20, 30 or 40 pmol of *PERK*-siRNA or *ATF6*-siRNA or with 40 pmol of scramble-siRNA (Scra) for 48 h. PERK and ATF6 protein expression was assessed by Western blotting. (B) BHK-21 cells were transfected with siRNA targeting *PERK* or Scra. After 48 h, the cells were infected with SVV and were further subjected to Western blotting to analyze the PERK, VP1, LC3 and β-actin expression levels at 24 hpi. Quantification shown with graphs representing the PERK/β-actin or VP1/β-actin ratios normalized to the control condition. (C) BHK-21 cells were transfected with siRNA targeting *ATF6* or Scra. Cells were processed as described in (B) and analyzed with anti-ATF6, anti-LC3, anti-VP1 and anti-β-actin antibodies at 24 hpi. Quantification shown with graphs representing the ATF6/β-actin or VP1/β-actin ratios normalized to the control condition. (D) BHK-21 cells were treated as described in (B). Virus titers were determined by a plaque assay at 24 hpi in BHK-21 cells. (E) BHK-21 cells were treated as described in (C). Virus titers were determined by a plaque assay at 24 hpi in BHK-21 cells. Error bars: means ± SDs of three independent experiments. Two-way ANOVA; $^*P < 0.05$, $^{**}P < 0.01$, $^{***}P < 0.001$ compared to the control group.

Appendix A. Supplementary data

Supplementary data to this article can be found online at https://doi.org/10.1016/j.virol.2019.08.029.

References

Alexander, D.E., Ward, S.L., Mizushima, N., Levine, B., Leib, D.A., 2007. Analysis of the role of autophagy in replication of herpes simplex virus in cell culture. J. Virol. 81, 12128–12134.

Alirezaei, M., Flynn, C.T., Wood, M.R., Harkins, S., Whitton, J.L., 2015. Coxsackievirus can exploit LC3 in both autophagy-dependent and -independent manners in vivo. Autophagy 11, 1389–1407.

Benali-Furet, N.L., Chami, M., Houel, L., De Giorgi, F., Vernejoul, F., Lagorce, D., Buscail, L., Bartenschlager, R., Ichas, F., Rizzuto, R., Paterlini-Bréchot, P., 2005. Hepatitis C virus core triggers apoptosis in liver cells by inducing ER stress and ER calcium depletion. Oncogene 24, 4921–4933.

Boya, P., González-Polo, R.A., Casares, N., Perfettini, J.L., Dessen, P., Larochette, N., Métivier, D., Meley, D., Souquere, S., Yoshimori, T., Pierron, G., Codogno, P., Kroemer, G., 2005. Inhibition of macroautophagy triggers apoptosis. Mol. Cell. Biol. 25, 1025–1040.

Canning, P., Canon, A., Bates, J.L., Gerardy, K., Linhares, D.C., Piñeyro, P.E., Schwartz, K.J., Yoon, K.J., Rademacher, C.J., Holtkamp, D., Karriker, L., 2016. Neonatal mortality, vesicular lesions and lameness associated with Senecavirus A in a U.S. sow farm. Transbound. Emerg. Dis. 63, 373–378.

Coffin, R.S., 2015. From virotherapy to oncolytic immunotherapy: where are we now? Curr. Opin. Virol. 13, 93–100.

Corona, A.K., Saulsbery, H.M., Corona Velazquez, A.F., Jackson, W.T., 2018. Enteroviruses remodel autophagic trafficking through regulation of host SNARE proteins to promote virus replication and cell exit. Cell Rep. 22, 3304–3314.

Corona Velazquez, A., Corona, A.K., Klein, K.A., Jackson, W.T., 2018. Poliovirus induces autophagic signaling independent of the ULK1 complex. Autophagy 14, 1201–1213.

Fan, X., Han, S., Yan, D., Gao, Y., Wei, Y., Liu, X., Liao, Y., Guo, H., Sun, S., 2017. Foot-and-mouth disease virus infection suppresses autophagy and NF-small ka, CyrillicB antiviral responses via degradation of ATG5-ATG12 by 3C(pro). Cell Death Dis. 8, e2561.

Fu, Y., Xu, W., Chen, D., Feng, C., Zhang, L., Wang, X., Lv, X., Zheng, N., Jin, Y., Wu, Z., 2015. Enterovirus 71 induces autophagy by regulating has-miR-30a expression to promote viral replication. Antivir. Res. 124, 43–53.

García-Valtanen, P., Ortega-Villaizán Mdel, M., Martínez-López, A., Medina-Gali, R., Pérez, L., Mackenzie, S., Figueras, A., Coll, J.M., Estepa, A., 2014. Autophagy-inducing peptides from mammalian VSV and fish VHSV rhabdoviral G glycoproteins (G) as models for the development of new therapeutic molecules. Autophagy 10, 1666–1680.

Gladue, D.P., O'Donnell, V., Baker-Branstetter, R., Holinka, L.G., Pacheco, J.M., Fernandez-Sainz, I., Lu, Z., Brocchi, E., Baxt, B., Piccone, M.E., Rodriguez, L., Borca, M.V., 2012. Foot-and-mouth disease virus nonstructural protein 2C interacts with Beclin1, modulating virus replication. J. Virol. 86, 12080–12090.

Hales, L.M., Knowles, N.J., Reddy, P.S., Xu, L., Hay, C., Hallenbeck, P.L., 2008. Complete genome sequence analysis of Seneca Valley virus-001, a novel oncolytic picornavirus. J. Gen. Virol. 89, 1265–1275.

Haze, K., Yoshida, H., Yanagi, H., Yura, T., Mori, K., 1999. Mammalian transcription factor ATF6 is synthesized as a transmembrane protein and activated by proteolysis in response to endoplasmic reticulum stress. Mol. Biol. Cell 10, 3787–3799.

Hou, L., Ge, X., Xin, L., Zhou, L., Guo, X., Yang, H., 2014. Nonstructural proteins 2C and 3D are involved in autophagy as induced by the encephalomyocarditis virus. Virol. J. 11, 156.

Hou, L., Wei, L., Zhu, S., Wang, J., Quan, R., Li, Z., Liu, J., 2017. Avian metapneumovirus subgroup C induces autophagy through the ATF6 UPR pathway. Autophagy 13, 1709–1721.

Hu, B., Zhang, Y., Jia, L., Wu, H., Fan, C., Sun, Y., Ye, C., Liao, M., Zhou, J., 2015. Binding of the pathogen receptor HSP90AA1 to avibirnavirus VP2 induces autophagy by inactivating the AKT-MTOR pathway. Autophagy 11, 503–515.

Joshi, L.R., Fernandes, M.H., Clement, T., Lawson, S., Pillatzki, A., Resende, T.P., Vannucci, F.A., Kutish, G.F., Nelson, E.A., Diel, D.G., 2016a. Pathogenesis of Senecavirus A infection in finishing pigs. J. Gen. Virol. 97, 3267–3279.

Joshi, L.R., Mohr, K.A., Clement, T., Hain, K.S., Myers, B., Yaros, J., Nelson, E.A., Christopher-Hennings, J., Gava, D., Schaefer, R., Caron, L., Dee, S., Diel, D.G., 2016b. Detection of the emerging picornavirus Senecavirus A in pigs, mice, and houseflies. J. Clin. Microbiol. 54, 1536–1545.

Kabeya, Y., Mizushima, N., Ueno, T., Yamamoto, A., Kirisako, T., Noda, T., Kominami, E., Ohsumi, Y., Yoshimori, T., 2000. LC3, a mammalian homologue of yeast Apg8p, is localized in autophagosome membranes after processing. EMBO J. 19, 5720–5728.
Kania, E., Pajak, B., Orzechowski, A., 2015. Calcium homeostasis and ER stress in control of autophagy in cancer cells. BioMed Res. Int. 2015, 352794.
Klionsky, D.J., Abdelmohsen, K., Abe, A., et al., 2016. Guidelines for the use and interpretation of assays for monitoring autophagy (third ed.). Autophagy 12, 1–222.
Klionsky, D.J., Abeliovich, H., Agostinis, P., et al., 2008. Guidelines for the use and interpretation of assays for monitoring autophagy in higher eukaryotes. Autophagy 4, 151–175.
Komatsu, M., Waguri, S., Ueno, T., Iwata, J., Murata, S., Tanida, I., Ezaki, J., Mizushima, N., Ohsumi, Y., Uchiyama, Y., Kominami, E., Tanaka, K., Chiba, T., 2005. Impairment of starvation-induced and constitutive autophagy in Atg7-deficient mice. J. Cell Biol. 169, 425–434.
Leme, R.A., Alfieri, A.F., Alfieri, A.A., 2017. Update on Senecavirus infection in pigs. Viruses 9.
Leme, R.A., Oliveira, T.E., Alcântara, B.K., Headley, S.A., Alfieri, A.F., Yang, M., Alfieri, A.A., 2016. Clinical manifestations of Senecavirus A infection in neonatal pigs, Brazil, 2015. Emerg. Infect. Dis. 22, 1238–1241.
Liang, C., Lee, J.S., Inn, K.S., Gack, M.U., Li, Q., Roberts, E.A., Vergne, I., Deretic, V., Feng, P., Akazawa, C., Jung, J.U., 2008. Beclin1-binding UVRAG targets the class C Vps complex to coordinate autophagosome maturation and endocytic trafficking. Nat. Cell Biol. 10, 776–787.
Liu, B., Fang, M., Hu, Y., Huang, B., Li, N., Chang, C., Huang, R., Xu, X., Yang, Z., Chen, Z., Liu, W., 2014. Hepatitis B virus X protein inhibits autophagic degradation by impairing lysosomal maturation. Autophagy 10, 416–430.
Meng, C., Zhou, Z., Jiang, K., Yu, S., Jia, L., Wu, Y., Liu, Y., Meng, S., Ding, C., 2012. Newcastle disease virus triggers autophagy in U251 glioma cells to enhance virus replication. Arch. Virol. 157, 1011–1018.
Mizushima, N., Yamamoto, A., Hatano, M., Kobayashi, Y., Kabeya, Y., Suzuki, K., Tokuhisa, T., Ohsumi, Y., Yoshimori, T., 2001. Dissection of autophagosome formation using Apg5-deficient mouse embryonic stem cells. J. Cell Biol. 152, 657–668.
Mizushima, N., Yoshimori, T., 2007. How to interpret LC3 immunoblotting. Autophagy 3, 542–545.
Mizushima, N., Yoshimori, T., Levine, B., 2010. Methods in mammalian autophagy research. Cell 140, 313–326.
Mohamud, Y., Qu, J., Xue, Y., Liu, H., Deng, H., Luo, H., 2019. CALCOCO2/NDP52 and SQSTM1/p62 differentially regulate coxsackievirus B3 propagation. Cell Death Differ. 26, 1062–1076.
Noda, T., Ohsumi, Y., 1998. Tor, a phosphatidylinositol kinase homologue, controls autophagy in yeast. J. Biol. Chem. 273, 3963–3966.
Pasma, T., Davidson, S., Shaw, S.L., 2008. Idiopathic vesicular disease in swine in Manitoba. Can. Vet. J. 49, 84–85.
Saeng-Chuto, K., Rodtian, P., Temeeyasen, G., Wegner, M., Nilubol, D., 2018. The first detection of Senecavirus A in pigs in Thailand, 2016. Transbound. Emerg. Dis. 65, 285–288.
Shen, J., Chen, X., Hendershot, L., Prywes, R., 2002. ER stress regulation of ATF6 localization by dissociation of BiP/GRP78 binding and unmasking of Golgi localization signals. Dev. Cell 3, 99–111.
Sir, D., Tian, Y., Chen, W.L., Ann, D.K., Yen, T.S., Ou, J.H., 2010. The early autophagic pathway is activated by hepatitis B virus and required for viral DNA replication. Proc. Natl. Acad. Sci. U. S. A. 107, 4383–43888.
Song, S., Tan, J., Miao, Y., Zhang, Q., 2018. Crosstalk of ER stress-mediated autophagy and ER-phagy: involvement of UPR and the core autophagy machinery. J. Cell. Physiol. 233, 3867–3874.
Sun, D., Vannucci, F., Knutson, T.P., Corzo, C., Marthaler, D.G., 2017. Emergence and whole-genome sequence of Senecavirus A in Colombia. Transbound. Emerg. Dis. 64, 1346–1349.
Tanida, I., 2011. Autophagosome formation and molecular mechanism of autophagy. Antioxidants Redox Signal. 14, 2201–2214.
Vannucci, F.A., Linhares, D.C., Barcellos, D.E., Lam, H.C., Collins, J., Marthaler, D., 2015. Identification and complete genome of Seneca Valley virus in vesicular fluid and sera of pigs affected with idiopathic vesicular disease, Brazil. Transbound. Emerg. Dis. 62, 589–593.
Wang, J., Kang, R., Huang, H., Xi, X., Wang, B., Wang, J., Zhao, Z., 2014. Hepatitis C virus core protein activates autophagy through EIF2AK3 and ATF6 UPR pathway-mediated MAP1LC3B and ATG12 expression. Autophagy 10, 766–784.
Yamamoto, A., Tagawa, Y., Yoshimori, T., Moriyama, Y., Masaki, R., Tashiro, Y., 1998. Bafilomycin A1 prevents maturation of autophagic vacuoles by inhibiting fusion between autophagosomes and lysosomes in rat hepatoma cell line, H-4-II-E cells. Cell Struct. Funct. 23, 33–42.
Yoon, S.Y., Ha, Y.E., Choi, J.E., Ahn, J., Lee, H., Kweon, H.S., Lee, J.Y., Kim, D.H., 2008. Coxsackievirus B4 uses autophagy for replication after calpain activation in rat primary neurons. J. Virol. 82, 11976–11978.
Yorimitsu, T., Nair, U., Yang, Z., Klionsky, D.J., 2006. Endoplasmic reticulum stress triggers autophagy. J. Biol. Chem. 281, 30299–30304.
Yoshimori, T., 2010. How autophagy saves mice: a cell-autonomous defense system against Sindbis virus infection. Cell Host Microbe 7, 83–84.
Yu, C.Y., Hsu, Y.W., Liao, C.L., Lin, Y.L., 2006. Flavivirus infection activates the XBP1 pathway of the unfolded protein response to cope with endoplasmic reticulum stress. J. Virol. 80, 11868–11880.
Zhang, Y., Li, Z., Ge, X., Guo, X., Yang, H., 2011. Autophagy promotes the replication of encephalomyocarditis virus in host cells. Autophagy 7, 613–628.
Zhang, H.M., Ye, X., Su, Y., Yuan, J., Liu, Z., Stein, D.A., Yang, D., 2010. Coxsackievirus B3 infection activates the unfolded protein response and induces apoptosis through downregulation of p58IPK and activation of CHOP and SREBP1. J. Virol. 84, 8446–8459.
Zhao, X., Wu, Q., Bai, Y., Chen, G., Zhou, L., Wu, Z., Li, Y., Zhou, W., Yang, H., Ma, J., 2017. Phylogenetic and genome analysis of seven senecavirus A isolates in China. Transbound. Emerg. Dis. 64, 2075–2082.
Zhu, Z., Yang, F., Chen, P., Liu, H., Cao, W., Zhang, K., Liu, X., Zheng, H., 2017. Emergence of novel Seneca Valley virus strains in China, 2017. Transbound. Emerg. Dis. 64, 1024–1029.
Zhu, G., Zheng, Y., Zhang, L., Shi, Y., Li, W., Liu, Z., Peng, B., Yin, J., Liu, W., He, X., 2013. Coxsackievirus A16 infection triggers apoptosis in RD cells by inducing ER stress. Biochem. Biophys. Res. Commun. 441, 856–861.